

---

# Repositioning of cells by mechanotaxis on surfaces with micropatterned Young's modulus

---

Darren S. Gray, Joe Tien, Christopher S. Chen

Department of Biomedical Engineering, Johns Hopkins University School of Medicine,  
720 Rutland Avenue, Baltimore, Maryland 21205

Received 11 April 2002; revised 29 August 2002; accepted 23 September 2002

**Abstract:** Adherent cells are strongly influenced by the mechanical aspects of biomaterials, but little is known about the cellular effects of spatial variations in these properties. This work describes a novel method to produce polymeric cell culture surfaces containing micrometer-scale regions of variable stiffness. Substrates made of acrylamide or poly-(dimethylsiloxane) were patterned with 100- or 10- $\mu\text{m}$  resolution, respectively. Cells were cultured on fibronectin-coated acrylamide having Young's moduli of 34 kPa and 1.8 kPa, or fibronectin-coated PDMS having moduli of 2.5 MPa and 12 kPa. Over several days, NIH/3T3 cells and bovine pulmonary arterial endothelial cells accumulated preferentially on stiffer regions of substrates. The migration, not

proliferation, of cells in response to mechanical patterning (mechanotaxis) was responsible for the accumulation of cells on stiffer regions. Differential remodeling of extracellular matrix protein on stiff versus compliant regions was observed by immunofluorescence staining, and may have been responsible for the observed mechanotaxis. These results suggest that mechanically patterned substrates might provide a general means to study mechanotaxis, and a new approach to patterning cells. © 2003 Wiley Periodicals, Inc. *J Biomed Mater Res* 66A: 605–614, 2003

**Key words:** mechanotaxis; durotaxis; microfabrication; cell patterning; extracellular matrix

---

## INTRODUCTION

The dynamic nature of adhesions to the extracellular matrix (ECM) allows cells to migrate in response to signals such as gradients of soluble chemoattractants.<sup>1,2</sup> *In vivo*, these highly orchestrated movements can cause cells to migrate to specific compartments of the body and are a critical component of developmental patterning, wound healing, and lymphocyte targeting.<sup>3–5</sup> Although gradients of soluble factors generally organize the body plan,<sup>3</sup> cells appear to receive additional guidance from the insoluble ECM. Changes in bound adhesive ligands, topographical features, and stiffness across a substrate can all lead to guided migration of cells.<sup>6–9</sup> To understand these cues and use them for organizing engineered tissues, many approaches have been developed to pattern ECM ligands or topology on cell culture substrates.<sup>6,10</sup> When substrates are patterned with ECM-

coated regions and nonadhesive regions, cells only attach to the ECM-coated regions.<sup>11</sup> Cells exposed to a gradient of immobilized ECM proteins migrate up the gradient, a phenomenon known as haptotaxis.<sup>6,12</sup> Cells also organize and align in response to topological cues, including surface grooves that are only 14 nm deep.<sup>9</sup> The use of patterned adhesivity and topology to organize cells is now an accepted strategy in tissue engineering. In contrast to the maturity of engineering surface adhesivity and topology, methods for patterning the stiffness of culture substrates, and the resulting cellular response, are not well established.

Recent reports suggest that cells migrate preferentially towards stiffer surfaces.<sup>7,13</sup> In these studies of mechanotaxis, cells were cultured on a surface with one stiff and one compliant region.<sup>7,14</sup> Cells were seeded sparsely because migration strictly from the compliant to the stiff region was not observed in the presence of cell–cell contacts. Therefore, only a small number of cells were present at the interface, and mechanotaxis could be observed only on a cell-by-cell basis. As a result, the ability to study, quantitate, and control the phenomenon has been restricted. Based on the available data, several investigators have speculated that mechanically mediated migration could be generated by modulation of the integrin-containing

Correspondence to: C. Chen; e-mail: cchen@bme.jhu.edu  
Contract grant sponsor: Whitaker Foundation  
Contract grant sponsor: NIGMS; contract grant number: GM 60692  
Contract grant sponsor: Office of Naval Research  
Contract grant sponsor: DARPA

adhesions which join the cytoskeleton and the ECM.<sup>7,13</sup> Remarkably, these mechanosensing adhesions are able to assemble in proportion to forces applied either externally<sup>13</sup> or through contractions generated by actin–myosin interactions within the cell.<sup>15a,15b</sup> Nonetheless, the mechanism by which such adhesions might mediate mechanotaxis remains to be determined. There is a need for an experimental system in which substrate stiffness could be spatially patterned over a surface coated with uniform ECM density.

This work describes a method to make acrylamide or poly(dimethylsiloxane) (PDMS) surfaces patterned with micrometer-scale regions of stiff or compliant materials with similar surface chemistry. By presenting cells with many boundaries between stiff and compliant regions, we investigated mechanotaxis in a large population of cells. Fibroblasts or endothelial cells were plated uniformly on these substrates and monitored for several days.

## MATERIALS AND METHODS

### Cell culture and reagents

NIH/3T3 fibroblasts (3T3s, ATCC CRL-1658) and bovine pulmonary arterial endothelial cells (BPAECs, VEC Technologies, Rensselaer, NY) were cultured under 5% and 10% CO<sub>2</sub> atmospheres, respectively. All cells were cultured in Dulbecco's modified Eagle's media supplemented with 10% calf serum, 100 U/mL penicillin, and 100 µg/mL streptomycin (Life Technologies). Before plating on experimental substrates, cells were detached using 0.25% trypsin and 1 mM ethylenediaminetetraacetic acid (EDTA). In some experiments, cells were growth arrested by 10 µg/mL of mitomycin C (Sigma), which was left in the culture media for 2 h after cell seeding and removed by three washes as described.<sup>16</sup>

### Fabrication of acrylamide substrates

The PDMS molds used in the fabrication of acrylamide substrates [Fig. 1(a)] were formed as previously described.<sup>17</sup> Briefly, SU-8 photoresist was spin-coated on a silicon wafer, exposed to UV light through a mask, and developed to form a bas-relief "master." PDMS prepolymer (Sylgard 184, Dow Corning) with a base:cure ratio of 10:1 was poured over the master, cured, peeled from the master, and cut into 1-cm<sup>2</sup> pieces. Immediately after being oxidized for 5 min in a plasma cleaner, the PDMS mold was sealed against a standard glass microscope slide. Acrylamide I, consisting of vacuum-degassed 0.07% wt/vol *N,N'*-methylenebisacrylamide (NMBA), 9.93% wt/vol acrylamide, 2.5% wt/vol 2,2'-azobis(2-methylpropionamide)dihydrochloride (Azobis, Aldrich), and 10 mM HEPES in water at pH 8.5, was wicked into the voids formed between the glass and the PDMS, and cured with approximately 9 J/cm<sup>2</sup> of UV irradiation from a quartz mercury vapor

lamp. The PDMS mold was gently removed from acrylamide I and the supporting glass slide. Acrylamide II, consisting of vacuum-degassed 0.5% wt/vol NMBA, 9.5% wt/vol acrylamide, 2.5% wt/vol Azobis, and 10 mM HEPES in water at pH 8.5, was poured over acrylamide I and cured by UV light. The composite structure was peeled from the glass and soaked in 50 mM HEPES at pH 8.5 (HEPES) for >10 min. Human fibronectin was crosslinked to the substrate as previously described.<sup>18</sup> Briefly, the substrates were immersed in a solution of 0.05% wt/vol sulfosuccinimidyl-6-(4'-azido-2'-nitrophenylamino)hexanoate (Sulfo-SANPAH, Pierce) and 0.5% dimethylsulfoxide in HEPES, exposed to approximately 2 J/cm<sup>2</sup> of UV and visible irradiation from a germicidal lamp, re-immersed in fresh Sulfo-SANPAH, exposed again, washed twice with HEPES, and agitated under HEPES for 10 min. Substrates were then incubated in 0.1 mg/mL fibronectin overnight at 4°C and rinsed seven times with phosphate-buffered saline (PBS) before use. Two sample substrates were distorted perpendicular to their surfaces by at least 20 µm, using the sharp tip of a 20-gauge needle. Microscopic visualization of this test ensured that the two types of acrylamide were securely bonded, thus providing a no-slip boundary condition between stiff and compliant regions.

### Fabrication of PDMS substrates

To mechanically pattern PDMS substrates [Fig. 1(b)], an aqueous solution of 50% wt/vol sucrose was spin-coated for 1 min at 1000 rpm on a plasma-oxidized silicon wafer. PDMS I was formed by curing prepolymer with base:cure ratio of 10:1 against a prepatterned master as previously described.<sup>17</sup> PDMS I was then peeled from the master, cut into 1-cm<sup>2</sup> pieces, heated to 65°C, and placed patterned side down on the sucrose, also at 65°C. PDMS II, with a base:cure ratio of 50:1 or 10:1, was heated to 65°C and wicked into the voids formed between PDMS I and the sucrose. After the curing of PDMS II, the sucrose layer was dissolved in water, freeing the mechanically patterned substrates. After substrates were inverted and rinsed with ddH<sub>2</sub>O, 33 µg/mL of human fibronectin was adsorbed from solution for 1 h and rinsed three times with PBS. As with acrylamide substrates, sample PDMS substrates were distorted to observe a non-slip boundary condition between stiff and compliant regions.

To produce mechanically uniform replicas that matched the topology of mechanically patterned PDMS, patterned substrates were treated with a vapor of tridecafluoro-1,1,2-2-tetrahydrooctyl-1-trichlorosilane (United Chemical Technologies). Additional PDMS was poured over the original substrates, cured, and peeled from the original to form negative replicas. The process was repeated to form positive replicas of the negative templates.

### Measurement of Young's modulus

The Young's moduli of acrylamide and PDMS were measured by stretching unpatterned test substrates as previously described.<sup>18</sup> Briefly, each material was cast in the form of a strip measuring approximately 1 mm × 10 mm × 50

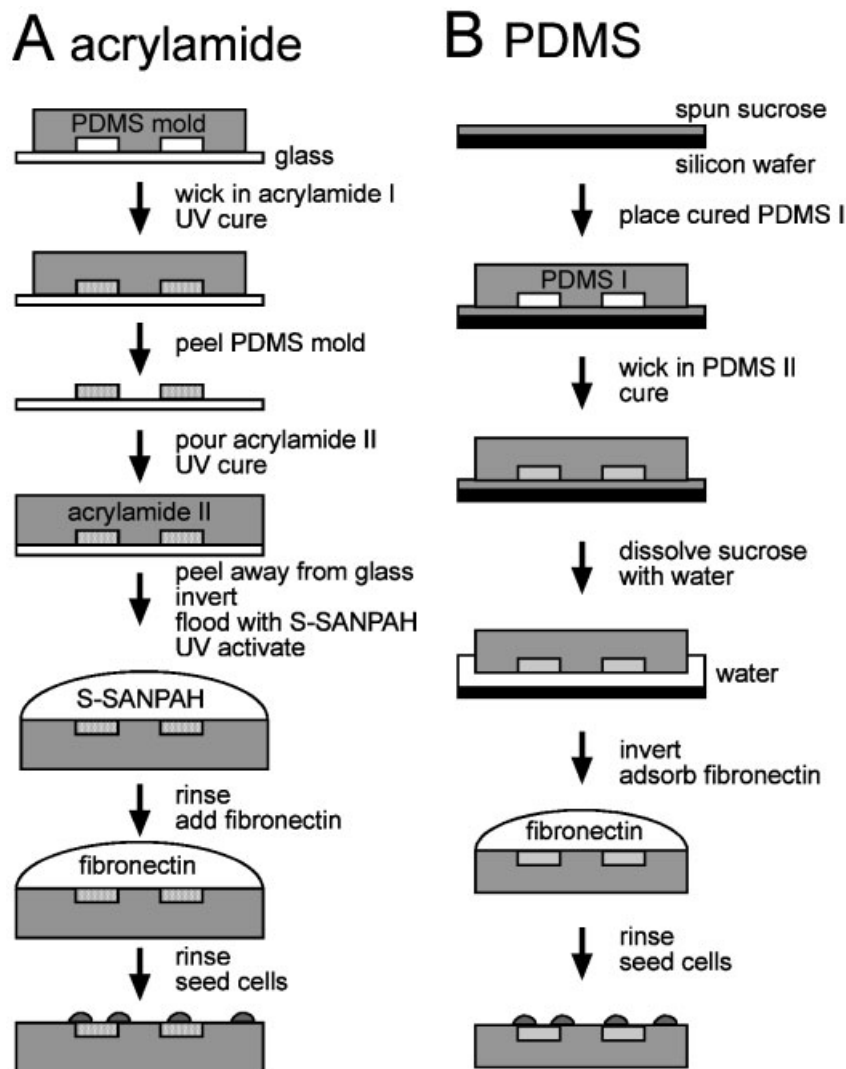


**Figure 1.** Schematic illustration of the procedure used to fabricate mechanically patterned substrates made of acrylamide (A) or PDMS (B). The micropatterned PDMS used as PDMS mold in (A) and as PDMS I in (B) was formed using a standard soft lithography techniques.

mm. These sheets were uniaxially deformed along their longest axis with the amount of tension required to produce a 5–30% strain. Tension was applied by suspended masses, typically 4 per substrate. Acrylamide samples were perfused with HEPES buffer between measurements. The stress–strain relationships were linear for the tested samples. Young’s modulus was calculated using the formula:  $E = (F/A)(L/\delta L)$ , where  $A$  = unstressed cross sectional area,  $F$  = force,  $L$  = unstressed length, and  $\delta L$  = change in length. The values reported are the averages of at least three samples of each type. Errors are standard error of the mean.

### Quantitation of cell accumulation

Phase contrast images of cells were taken using a cooled CCD camera (Spot RT Slider, Diagnostic Instruments) attached to an inverted microscope (Eclipse TE200, Nikon) with a 4× objective. Cells were counted manually from these images. Stiff

regions on PMDS substrates were clearly delimited as 500- × 500- $\mu\text{m}$  squares. Compliant regions of equal area were formed by the space between two adjacent squares. Cell density on stiff regions ( $D_s$ ) was calculated as a percentage of total cell density according to the formula:  $D_s = s/(s + c)$ , where  $s$  is the number of cells counted on two stiff regions per substrate and  $c$  is the number of cells counted on two compliant regions of equal area per substrate. Reported values are averages of 6 substrates per time point. In cases where substrates did not present a pattern, cells were counted in images representing 1- × 1.5-mm regions. This process was repeated three times for each substrate. Reported values are averages of four substrates of each type per time point. Statistical significance was determined using Student’s  $t$  test.

### Immunofluorescence staining

To detect fibronectin adsorbed on PDMS substrates, samples were fixed for 5 min in PBS containing 4% formalde-

hyde, washed three times in IF buffer (PBS containing 0.1 % BSA and 0.1% Triton X-100), and blocked for 30 min in IF buffer. Substrates were then incubated for 60 min in IF Buffer with 130  $\mu\text{g}/\text{mL}$  fluorescein-conjugated goat anti-human fibronectin antibody (#55193, ICN/Cappel) and then rinsed three times in IF buffer. Substrates were photographed using a cooled CCD camera attached to an inverted microscope with a 10 $\times$  objective. Images were then flat field corrected before plotting their intensity values using image-processing software (IPLab, Scanalytics).

## RESULTS

### Distribution of cells on mechanically patterned acrylamide substrates

Acrylamide hydrogels have been used previously to study cellular mechanotaxis by observing the preferential migration of individual cells at the interface of stiff and compliant regions.<sup>7</sup> To study this phenomenon on a population of cells, we first developed a method to fabricate acrylamide substrates with defined arrays of micrometer-scale regions [Fig. 1(a)]. To generate a layer of compliant acrylamide containing square holes, a mold was sealed against a glass slide before the acrylamide solution (acrylamide I) was flowed into the gaps between the mold and the glass. The acrylamide was cured and the mold removed, leaving a layer of polymerized acrylamide containing square holes. A second acrylamide solution (acrylamide II), containing a higher concentration of cross-linker, was then poured over the first acrylamide, filling in the square holes and forming the bulk of the substrate. After curing of the second acrylamide, the composite structure was peeled from the glass and flipped over, exposing an array of stiff acrylamide embedded with compliant acrylamide. Because the layer of acrylamide I was 175  $\mu\text{m}$  deep, and the distortions produced by cells were less than 1  $\mu\text{m}$ , the mechanical effect of the bulk underlayer of the substrate (made of acrylamide II) was assumed to be negligible at the surface of acrylamide I.

Feature sizes of 100  $\mu\text{m}$  and larger were easily achieved using 0.5% and 0.07% *N,N'*-methylenebisacrylamide cross-linker (NMBA) for stiff and compliant regions, respectively. A 10% concentration of total acrylamide (NMBA plus acrylamide) was used throughout these studies. Minimum feature size was limited largely by distortions in acrylamide I which occurred upon removal of the PDMS mold. Acrylamide substrates containing NMBA cross linker concentrations as low as 0.07% could be patterned; with lower crosslinker concentrations, the acrylamide tore during the fabrication process. When NMBA concentrations were increased to 1%, the acrylamide became cloudy and unsuitable for microscopic visualization.

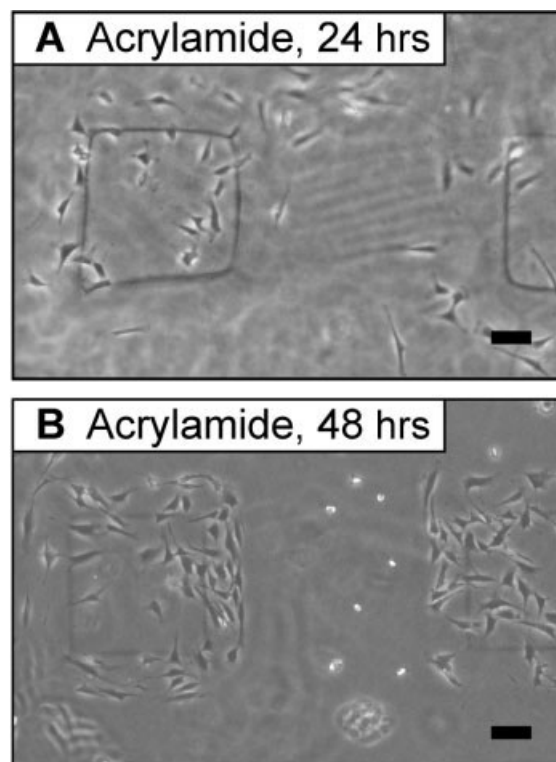


**Figure 2.** Cell accumulation on stiffer regions of acrylamide substances. Phase contrast images show cells on patterned substrates at 24 (A) and 48 h (B) after plating. In both pictures, the squares are stiff whereas the regions surrounding the squares are compliant. Scale bars represent 100  $\mu\text{m}$ .

To examine the behaviors of cells on these substrates, we coated their surfaces with fibronectin before seeding NIH/3T3 cells (3T3s). The two-acrylamide substrates contained regions with 0.5% and 0.07% NMBA cross linker concentrations. The Young's moduli of gels made with these cross-linker concentrations were measured to be  $34 \pm 3$  kPa and  $1.8 \pm 0.3$  kPa, respectively, with a linear stress-strain relationship up to at least 30% strain. We immersed the patterned substrates in culture media and plated 3T3s evenly across their surfaces. Cell distribution was monitored for several days after seeding. By three hours after seeding, the cells had attached to the entire substrate. Cell density was similar across both stiff and compliant regions, but cells were less spread on compliant regions, as observed in previous work.<sup>19</sup> Preferential accumulation of cells on stiff versus compliant areas was seen at 24 h after plating [Fig. 2(a)] and became more evident by 48 h [Fig. 2(b)]. Net migration towards stiff regions occurred in the presence of cell-cell contacts, in contrast to previous results.<sup>7</sup>

We found that the accumulation process was difficult to study using acrylamide substrates. The observed accumulation and general health of cells varied considerably. On occasion, cells did not accumulate over the observed time period. In other trials, the

stiffness of one or both substrates failed to support cell adhesion. Surface characterization of the immobilized protein and its interaction with the cells proved to be difficult with a hydrogel. Together, these characteristics made this approach unattractive for further study of the process of accumulation. To address the observed limitations, a method was developed to use PDMS, a silicone elastomer, as the substrate material.

### Distribution of cells on mechanically patterned PDMS substrates

Using a molding approach analogous to that used for patterning acrylamide, we fabricated PDMS substrates with defined arrays of square micrometer-scale regions of stiff PDMS next to more compliant PDMS [Fig. 1(b)]. PDMS (PDMS I) made with a high crosslinker concentration and patterned with raised square regions, was sealed against a flat layer of sucrose. A second PDMS (PDMS II) containing less crosslinker was flowed into the voids between the first PDMS and the sucrose. After curing PDMS II, the composite structure was released by dissolving the sucrose layer to expose a two-polymer surface. PDMS I and PDMS II, differing by their base:cross-linker ratios of 10:1 versus 50:1, were found to have Young's moduli of  $2.5 \pm 0.2$  MPa and  $12 \pm 1$  kPa, respectively, with a linear stress-strain relationship up to at least 30% strain. Because the layer of PDMS II was 175  $\mu\text{m}$  deep and the distortions produced by cells were less than 1  $\mu\text{m}$ , the mechanical effect of the bulk underlayer of the substrate (made of PDMS I) was assumed to be negligible at the surface of PDMS II. Without attempting to optimize pattern resolution, feature sizes of 10  $\mu\text{m}$  were achieved. Minimum feature size was related to the inability of smaller features in PDMS I to seal against the sucrose layer and exclude PDMS II from the culture surface.

To determine whether cells were influenced by the patterned stiffness of the substrate, we passively adsorbed fibronectin to the surface, seeded 3T3s, and monitored cell distribution for several days. BPAECs were cultured on PDMS during a single trial, which produced results similar to those obtained with the fibroblasts. Cells attached and spread on both stiff and compliant regions of substrates by 3 h after seeding. Cells appeared healthy on both stiff and compliant regions throughout the experiment. At 3 h, cell distribution appeared to be even, although slightly larger numbers of cells were counted on stiff areas [Fig. 3(a)]. This difference may have been caused by cell migration that occurred before the 3-h time point, or cells may have adhered preferentially to stiff regions. Accumulation of cells on stiff areas was typically seen at 24 h after plating [Fig. 3(b)] and became more evident

by 48 h [Fig. 3(c)]. As with acrylamide, net migration towards stiff regions occurred in the presence of cell-cell contact. The accumulation of cells on stiff regions appeared to coincide with a greater depletion on the compliant regions that were nearest to stiff areas, as compared to compliant areas farther from stiff areas. Such depletion suggests that cells near the boundaries between stiff and compliant zones detected the mechanical gradient and migrated to stiff regions. This finding contrasts with the accumulation of cells both on and near stiff regions of acrylamide, possibly indicating a more precise fabrication of stiff versus compliant areas on PDMS substrates. On a minority of PDMS substrates, cell distribution remained uniform. This variability appeared to stem from the manufacturing of the substrates, and these failed trials were excluded from quantitative analysis.

### Potential sources of preferential cell accumulation on stiff regions

The observed accumulation on stiff regions might have arisen from differences in proliferation on stiff versus compliant regions, preferential migration of cells from compliant to stiff regions, differences in migration speeds of compliant versus stiff regions, or a combination of factors. To eliminate any contribution of proliferation to the accumulation response, we blocked the division of cells with 10  $\mu\text{g}/\text{mL}$  of mitomycin C<sup>16</sup> and observed their behavior on patterned substrates. Overall, numbers of cells on these substrates did not change significantly for at least 5 days [Fig. 4(a)]. Accumulation on stiff areas was not seen at 2 days after plating, but by 5 days after plating, substrates showed clear accumulation [Fig. 4(b)]. This time-course of accumulation was slower than that observed with untreated cells on either acrylamide (Fig. 2) or PDMS (Fig. 3). To determine whether proliferation rates among normally dividing cells were different on stiff versus compliant regions, we plated untreated cells on uniform, unpatterned stiff, or compliant PDMS substrates. Cells were counted at 3 and 48 h after cell seeding. Over this time period, cells on uniformly stiff PDMS surfaces increased in number by  $4.9 \pm 0.4$  fold whereas cells on compliant surfaces increased by  $4.4 \pm 0.3$  fold. Taken together, these data suggest that the preferential accumulation of cells of stiff regions of patterned substrates arose primarily from cell migration, not differential proliferation.

With both acrylamide and PDMS substrates, we were unable to produce precisely planar surfaces. Compliant regions of acrylamide swelled relative to stiff regions due to osmotic forces. Compliant regions of PDMS shrank relative to stiff regions during polymerization. Because of the resulting gradually sloped

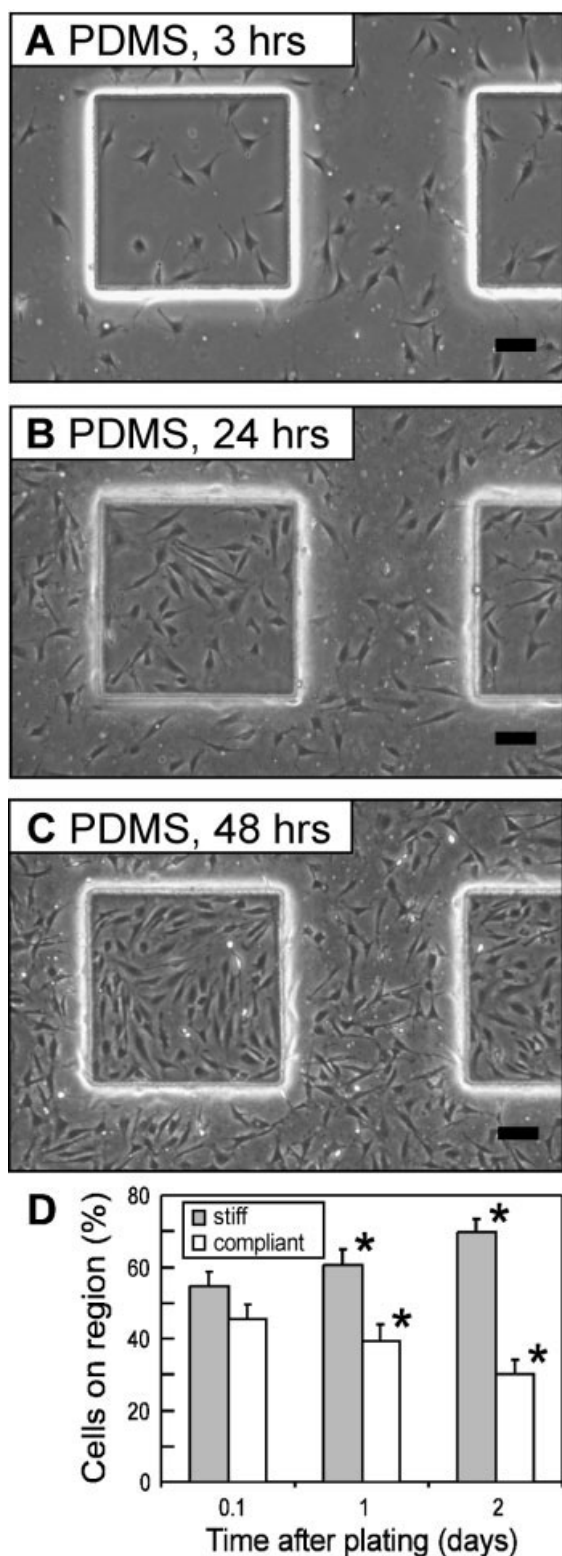


**Figure 3.** Cell accumulation on stiffer regions of PDMS substrates. A–C, Phase contrast images of cells on patterned PDMS substrates at the indicated times after plating. The squares are stiff whereas the regions surrounding the squares are compliant. D, Plot of the percentage of total cell density on stiff and compliant regions as a function of time after plating. Error bars are standard error of the mean ( $*p < 0/05$  vs other regions at the same point). Scale bars represent 100  $\mu\text{m}$ .

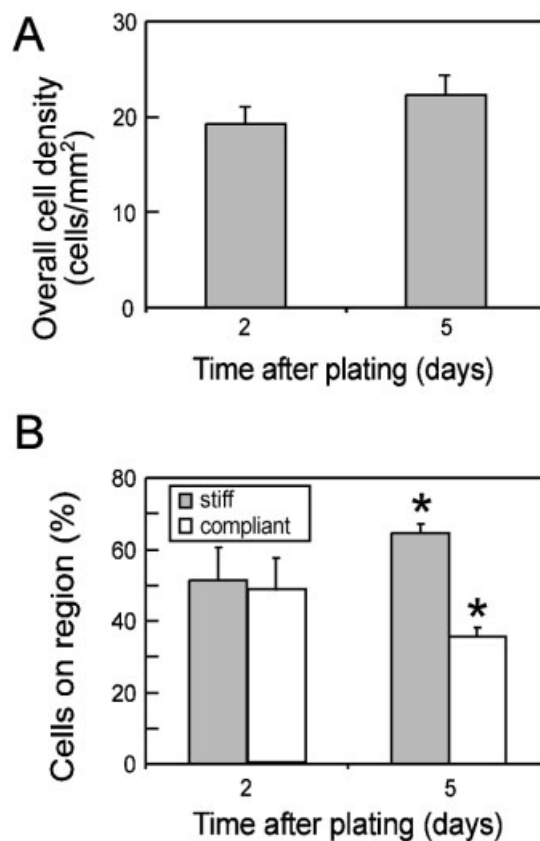


**Figure 4.** Cell accumulation without proliferation. A, Plot of cell density on patterned PDMS substrates versus time, with cell proliferation blocked by mitomycin C. Cell density is averaged over all substrate regions. B, Plot of the percentage of cell density on stiff and compliant regions of PDMS substrates versus time, with cell proliferation blocked by the addition of mitomycin C. Error bars are standard error of the mean ( $*p < 0.05$  vs 50% level).

depressions, the centers of compliant regions of PDMS were as much as 15  $\mu\text{m}$  out of the plane of the relatively flat stiff areas. Because cell orientation and migration have been shown to respond to step changes in substrate topology,<sup>20,21</sup> the accumulation observed in our experiments might have resulted from the topology of our substrates rather than differential stiffness. To assess this possibility, we made uniformly stiff substrates with surface profiles identical to the patterned substrates. Replicas made only of stiff PDMS were cast from the patterned, two-component PDMS substrates, forming an inverse topology of the original, patterned surfaces. Secondary replicas were then cast from these primary replicas by the same procedure, resulting in uniformly stiff substrates with the same topology as the patterned substrates. Cells plated on these PDMS replicas did not accumulate (data not shown). Therefore, the sloping topology of our mechanically patterned substrates was not the cause of cell migration to stiff areas. We cannot exclude the possibility that gradients of stiffness caused

cell accumulation only in the presence of topology. Although the imperfect flatness of the current substrates would hinder their applicability to some studies, it should be possible to produce highly planar surfaces with improved methods.

### ECM distribution and remodeling on patterned substrates

To determine whether uneven ECM coating of the substrates played a role in cellular patterning, we measured the amount of fibronectin present on the surfaces of the patterned substrates. Adsorbed fibronectin was assessed by immunolabeling with a fluorescein-conjugated anti-fibronectin antibody. Fluorescence images demonstrated that the initial distribution of fibronectin was relatively even across the substrate surface [Fig. 5(a,d)]. The subtle fluctuations in fluorescent staining showed no consistent relationship with stiff or compliant areas. Although fluorescence intensity is not a linear indicator of the amount of fibronectin, quantitative radiolabeling studies have shown that fluorescence intensity increases with surface density of fibronectin.<sup>22</sup> Thus, the initial concentration of adsorbed fibronectin probably did not cause the observed migration to stiff PDMS.

The fibronectin on stiff regions might also have been more stable over time than fibronectin on compliant regions. Given that accumulation took place over several days, we examined PDMS substrates subjected to the tissue culture environment for 48 h with or without cells. In the absence of cells, fibronectin adsorbed on substrates remained stable and evenly distributed [Fig. 5(b,e)]. In contrast, fibronectin distribution became uneven on substrates cultured with cells for 48 h [Fig. 5(c)]. On compliant regions, the intensity of staining increased near cells and decreased elsewhere. The change in fibronectin distribution suggested that cells may have participated in active ECM remodeling in compliant regions. On stiff regions, fibronectin staining increased only in the exact locations of cells. In areas not occupied by cells, levels remained unchanged relative to those seen on cell-free substrates. A comparison of fibronectin levels on representative cell-free areas from substrates before tissue culture, after exposure to tissue culture conditions without cells, or after culture with cells demonstrates that fibronectin levels remained stable on stiff regions under all conditions. In contrast, the compliant regions of the substrate seeded with cells underwent a dramatic reduction in ECM density relative to cell-free substrates [Fig. 5(f)]. These observations imply that significant, cell-dependent remodeling of the fibronectin occurred only on the compliant regions. Although the mechanism remains uncertain, this differential remodeling

may be either a result or a critical component of mechanotaxis.

## DISCUSSION

We have demonstrated the preferential accumulation of cells on stiff regions of mechanically patterned acrylamide and PDMS substrates. The ability to observe mechanotaxis on a large population over long time scales now enables a statistical approach to studying the phenomenon, and complements the cell-by-cell, time-lapse observations that first reported mechanotaxis. For example, previous studies found that, although isolated cells were able to migrate only from compliant to stiff regions, cells with neighbors were able to migrate from stiff to compliant regions as well.<sup>7</sup> However, because of the short time scale of these studies and the lack of population data, it was unclear what the net effect would be on the whole population. Our experiments show that thousands of cells accumulated over several days on each substrate even in the presence of many cell-cell contacts. Thus, over a sufficiently long time span and averaged over many cells, a net migration toward stiff regions did occur.

Although previous studies of mechanotaxis have used acrylamide substrates,<sup>7,23</sup> we found PDMS to have several advantages. The 10- $\mu\text{m}$  resolution of patterning using PDMS was significantly better than the 100- $\mu\text{m}$  features produced with acrylamide. Accumulation on acrylamide substrates was not restricted only to the stiff regions; the area of cell accumulation also included a border zone extending approximately 100  $\mu\text{m}$  into the compliant regions. This effect might indicate that the transition from stiff to compliant surface did not occur as a simple step function at the interfacial boundary. For example, the higher concentration of crosslinker in stiff regions could diffuse into nearby compliant regions during the fabrication process (consistent with literature on small molecule diffusion in acrylamide gels).<sup>24,25</sup> Diffusion of crosslinker could have shifted the stiff-compliant boundary or created a more gradual transition in substrate stiffness. With PDMS, cells accumulated strictly on stiff regions, facilitating straightforward quantitation and interpretation. Such analysis would have been more difficult on acrylamide substrates, where the boundary between stiff and compliant may have shifted or blurred. In addition, tools to coat PDMS with a protein or otherwise modify its surface are relatively well established.<sup>26,27</sup> Such tools could facilitate simultaneous chemical (ECM protein) and mechanical patterning of substrates. Because PDMS has a definitive interface between substrate and aqueous solution, its surface can be easily characterized using standard surface

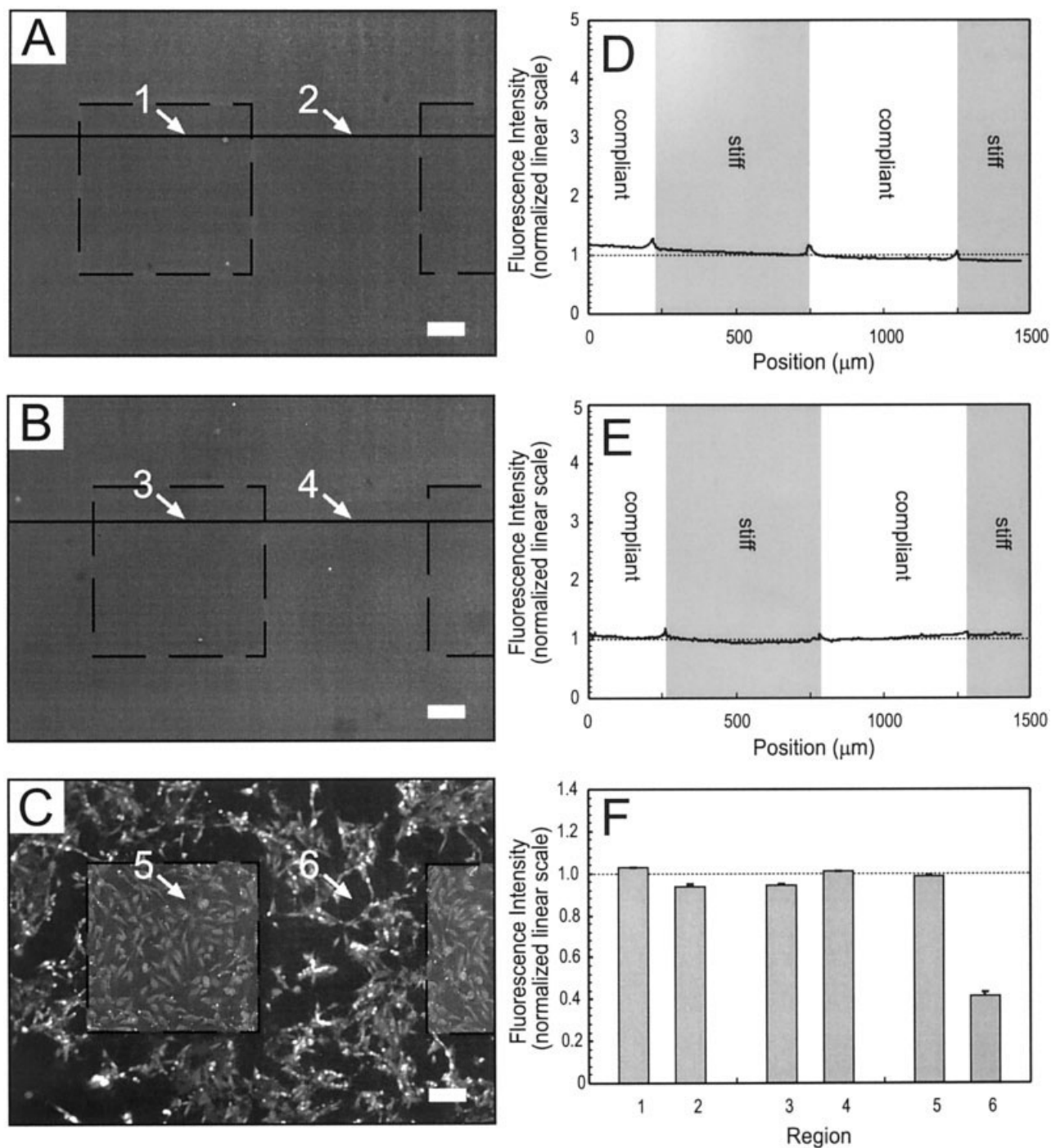


**Figure 5.** Immunofluorescence staining for fibronectin. A, Fluorescence image of substrate stained for fibronectin after a 5-min exposure to tissue culture conditions without cells. B, Fluorescence image of substrate stained for fibronectin after 48 h in tissue culture conditions without cells. C, Fluorescence image of substrate stained for fibronectin after 3T3s were cultured for 48 h. Cells are visible because of staining of intracellular fibronectin. Dotted lines in the images indicate the stiff/compliant boundaries. D and E, Fluorescence intensity of antifibronectin antibody plotted versus position along the corresponding images in (A) and (B), respectively. Fluorescence intensity was quantitated by the average fluorescence intensity along the 10- $\mu\text{m}$  wide paths centered on the solid lines in (A) and (B) and normalized to the fluorescence intensity on portions of the stiff regions not occupied by cells. F, Graph of the average intensity of representative regions 1 through 6 indicated in (A)–(C). Each region is 100  $\mu\text{m}^2$ , centered about the tip of the arrow that points to it. Error bars are standard error of the mean. Scale bars represent 100  $\mu\text{m}$ .

analysis, while the hydrated acrylamide would require specialized approaches.<sup>7</sup> In our study, this was evidenced by the use of immunofluorescence tech-

niques to study ECM remodeling. Staining only the surface of acrylamide was impossible because antibodies permeated and stained the entire substrate; we

could not isolate and observe the ECM at the cell-substrate boundary.

After selecting PDMS as the preferred substrate material, we further evaluated the preferential accumulation. As shown by other groups, cells may adhere more strongly and spread to greater areas on stiff versus compliant surfaces.<sup>13,19</sup> Because differences in cell adhesion can influence rates of cell division,<sup>28</sup> we investigated the possibility that cells accumulated on stiff regions of PDMS based on greater rates of cell division. Our finding that cell proliferation rates were comparable on stiff versus compliant substrates, and that cells treated with mitomycin C still accumulated on stiff regions, suggests that mechanotaxis, and not differential proliferation, was responsible for the observed accumulation. The slower rates of accumulation seen when proliferation was blocked may have resulted from mitomycin C-induced toxicity.<sup>29</sup>

Analysis of the distribution of bound fibronectin on patterned surfaces was prompted by previous demonstrations that cells cultured on gradients of ECM density can undergo haptotaxis, the migration towards higher surface densities of bound ECM molecules.<sup>6</sup> Immunostaining revealed initially uniform protein distribution, which was then altered only in the presence of cells. These ECM changes could have been either a cause or result of cell migration.<sup>30</sup> Mechanical stresses, caused by traction forces of adherent cells, might have differed between stiff and compliant regions. Such stresses could have regulated the cellular production and degradation of proteins or differentially disrupted the ECM on the compliant versus stiff regions.<sup>30–32</sup> Thus, cells might have locally depleted the ECM on compliant regions, causing migration onto the stable, stiff regions via haptotaxis. Alternatively, the observed changes in the ECM might have been an outcome of mechanotaxis, rather than a cause of migration. Because motility itself can increase ECM remodeling,<sup>18</sup> the increased motility during mechanotaxis of cells on compliant regions could have caused the fibronectin redistribution we observed. The current study did not address the possibility that subtle differences in surface chemistry of stiff versus compliant regions of the substrates may exist that directly affect cell adhesion, alter fibronectin conformation, or differently adsorb components of serum.<sup>22</sup>

Mechanically patterned substrates will be valuable tools for the investigation of cellular phenomena that potentially depend on substrate stiffness, including mechano-transduction, embryological development, and wound healing. The high density of patterned features on the surfaces facilitates rapid, quantitative analysis of cell distributions. The high percentage of cells near boundaries is expected to amplify any mechanically induced behaviors and reduce statistical fluctuations associated with cells unaffected by distant mechanical gradients. Because features of 10  $\mu\text{m}$  and

potentially smaller can be patterned, stiffness can be controlled on an appropriate size scale for evaluation of subcellular responses such as the mechanosensing role of individual focal adhesions.<sup>33–35</sup> Ultimately, such studies could help to elucidate the mechanisms by which cells sense and respond to their mechanical environment.

Mechanical patterning might provide an alternative to chemical patterning<sup>17,36</sup> as a means to organize cells on a substrate. The two methods produce different types of responses. For example, the time courses of patterning cells vary significantly. If mediated by chemical adhesivity, the organization of cells on the surface occurs in minutes to hours, when cells actively adhere to the defined pattern.<sup>11</sup> In the case of mechanical patterning, the cells distribute uniformly over the surface and then reposition themselves gradually over several days. The time course of decay may also vary between the two types of patterning. Using substrate stiffness to guide cell migration could facilitate long-term patterning of cell cultures by overcoming the gradual degradation often seen when patterned surface chemistries interact with biological environments.<sup>37</sup> These features of the mechanical approach may be useful for some applications. Although more than 95% accumulation on desired regions is routinely achieved with chemical patterning, only 70% accumulation was seen in this study using mechanical patterning. However, the unoptimized substrates used here were patterned with one pair of stiffness, the widest range of stiffness conveniently achievable with the polymers used. In future studies, the extent of mechanical patterning might be improved by examining different parameters of stiffness and gradients of stiffness.

Because substrate stiffness and surface chemistry can be controlled independently, more complicated distributions of adherent cells might be achieved by simultaneously employing the two orthogonal guidance cues. For example, nonmigratory cell types might attach only to adhesive regions superimposed on a mechanically patterned substrate but remain unaffected by the mechanical pattern. Migratory cells such as those used in our experiments could be co-cultured on the same substrates but localize to a subset of the adhesive regions as they migrate to stiff areas.

## CONCLUSIONS

We have developed and tested mechanically patterned, polymeric, cell-culture substrates. Preferential cell accumulation on stiffer regions produced a simple, graphical demonstration of mechanotaxis in the presence of cell–cell contact. This phenomenon was shown to be a potential patterning tool that is able to

organize cells over several days. On PDMS substrates, migration was correlated with increased cell-mediated remodeling and depletion of ECM molecules on compliant versus stiff regions. The apparent occurrence of mechanotaxis in this study suggests that the phenomenon could play an important role *in vivo*, and could be used in patterning applications.

The authors thank John Tan, Celeste Nelson, Yu-Li Wang, and Alan Cheshire for stimulating discussions and technical suggestions.

## References

- Boyden S. The chemotactic effect of mixtures of antibody and antigen on polymorphonuclear leucocytes. *J Exp Med* 1962; 115:453–466.
- Stossel TP. On the crawling of animal cells. *Science* 1993;260: 1086–1094.
- Krumlauf R. *Hox* genes in vertebrate development. *Cell* 1994; 78: 191–201.
- Mast BA, Schultz GS. Interactions of cytokines, growth factors and proteases in acute and chronic wounds. *Wound Repair Regen* 1996;20:411–420.
- Springer TA. Traffic signals for lymphocyte recirculation and leukocyte emigration: the multistep paradigm. *Cell* 1994;76: 301–314.
- Brandley BK, Schnaar RL. Tumor cell haptotaxis on covalently immobilized linear and exponential gradients of a cell adhesion peptide. *Dev Biol* 1989;135:74–86.
- Lo CM, Wang HB, Dembo M, Wang YL. Cell Movement Is Guided by the Rigidity of the Substrate. *Biophys J* 2000;79: 144–152.
- Mandeville JT, Lawson MA, Maxfield FR. Dynamic imaging of neutrophil migration in three dimensions: mechanical interactions between cells and matrix. *J Leukoc Biol* 1997;61:188–200.
- Rajnicek A, Britland S, McCaig C. Contact guidance of CNS neurites on grooved quartz: influence of groove dimensions, neuronal age and cell type. *J Cell Sci* 1997;110:2905–2913.
- Curtis A, Wilkinson C. Topographical control of cells. *Biomaterials* 1997;18: 1573–1583.
- Chen CS, Mrksich M, Huang S, Whitesides GM, Ingber DE. Micropatterned surfaces for control of cell shape, position, and function. *Biotechnol Prog* 1998;14:356–363.
- Carter SB. Haptotaxis and the mechanism of cell motility. *Nature* 1967;213:256–260.
- Choquet D, Felsenfeld DP, Sheetz MP. Extracellular matrix rigidity causes strengthening of integrin-cytoskeleton linkages. *Cell* 1997;88:39–48.
- Wang HB, Dembo M, Hanks SK, Wang YL. Focal adhesion kinase is involved in mechanosensing during fibroblast migration. *Proc Natl Acad Sci USA* 2001;98:11295–11300.
- a) Balaban NQ, Schwarz US, Rivelino D, Goichberg P, Tzur G, Sabanay I, Mahalu D, Safran S, Bershadsky A, Addadi L, Geiger B. Force and focal adhesion assembly: a close relationship studied using elastic micropatterned substrates. *Nat Cell Biol* 2001;3:466–472; b) Tan JL, Tien J, Pirone D, Gray DS, Chen CS. Cells lying on a bed of microneedles: An approach to isolate mechanical force. *Proc Natl Acad Sci USA* 2003;100: 1484–1489.
- Bhatia SN, Balis UJ, Yarmush ML, Toner M. Microfabrication of hepatocyte/fibroblast co-cultures: role of homotypic cell interactions. *Biotechnol Prog* 1998;14: 378–387.
- Kane RS, Takayama S, Ostuni E, Ingber DE, Whitesides GM. Patterning proteins and cells using soft lithography. *Biomaterials* 1999;20:2363–2376.
- Pelham RJ Jr, Wang YL. Cell locomotion and focal adhesions are regulated by substrate flexibility. *Proc Natl Acad Sci USA* 1997;94:13661–13665.
- Thomas TW, DiMilla PA. Spreading and motility of human glioblastoma cells on sheets of silicone rubber depend on substratum compliance. *Med Biol Eng Comput* 2000;38:360–370.
- Tan J, Shen H, Saltzman WM. Micron-Scale Positioning of Features Influences the Rate of Polymorphonuclear Leukocyte Migration. *Biophys J* 2001;81: 2569–2579.
- Curtis AS, Wilkinson CD. Reactions of cells to topography. *J Biomater Sci Polym Ed* 1998;9:1313–1329.
- Garcia AJ, Vega MD, Boettiger D. Modulation of cell proliferation and differentiation through substrate-dependent changes in fibronectin conformation. *Mol Biol Cell* 1999;10:785–798.
- Wang HB, Dembo M, Wang YL. Substrate flexibility regulates growth and apoptosis of normal but not transformed cells. *Am J Physiol Cell Physiol* 2000;279:C1345–1350.
- Dickson RM, Norris DJ, Tzeng YL, Moerner WE. Three-dimensional imaging of single molecules solvated in pores of poly-(acrylamide) gels. *Science* 1996;274:966–969.
- Brody J, Yager P, Goldstein R, Austin R. Biotechnology at low Reynolds numbers. *Biophys. J.* 1996;71:3430–3441.
- Wang YL, Pelham RJ Jr. Preparation of a flexible, porous polyacrylamide substrate for mechanical studies of cultured cells. *Methods Enzymol* 298:489–496.
- Tan JT, Tien J, Chen CS. Microcontact printing of proteins on mixed self-assembled monolayers. *Langmuir* 2001;18:519–523.
- Danen EH, Yamada KM. Fibronectin, integrins, and growth control. *J Cell Physiol* 2001;189:1–13.
- Tomasz M, Lipman R, Chowdary D, Pawlak J, Verdine GL, Nakanishi K. Isolation and structure of a covalent cross-link adduct between mitomycin C and DNA. *Science* 1987;235: 1204–1208.
- Stopak D, Harris AK. Connective tissue morphogenesis by fibroblast traction. I. Tissue culture observations. *Dev Biol* 1982;90:383–398.
- Chiquet M, Matthisson M, Koch M, Tannheimer M, Chiquet-Ehrismann R. Regulation of extracellular matrix synthesis by mechanical stress. *Biochem Cell Biol* 1996;74:737–744.
- Kessler D, Dethlefsen S, Haase I, Plomann M, Hirche F, Krieg T, Eckes B. Fibroblasts in mechanically stressed collagen lattices assume a “synthetic” phenotype. *J Biol Chem* 2001;276: 36575–36585.
- Geiger B, Bershadsky A. Assembly and mechanosensory function of focal contacts. *Curr Opin Cell Biol* 2001;13:584–592.
- Sawada Y, Sheetz MP. Force transduction by Triton cytoskeletons. *J Cell Biol* 2002;156:609–615.
- Ingber DE. Integrins as mechanochemical transducers. *Curr Opin Cell Biol* 1991;3:841–848.
- Bhatia SN, Yarmush ML, Toner M. Controlling cell interactions by micropatterning in co-cultures: hepatocytes and 3T3 fibroblasts. *J Biomed Mater Res* 1997;34:189–199.
- Roberts C, Chen CS, Mrksich M, Martichonok V, Ingber DE, Whitesides GM. Using mixed self-assembled monolayers presenting RGD and (EG)3OH groups to characterize long-term attachment of bovine capillary endothelial cells to surfaces. *J Am Chem Soc* 1998;120:6548–6555.